Zoomorphology (2018) 137:177–190
https://doi.org/10.1007/s00435-017-0373-8

ORIGINAL PAPER

Light and electron microscopic studies on the retina of the booted eagle (*Aquila pennata*)

Y. G. Montoyo[1] · M. García[1] · Yolanda Segovia[1]

Received: 10 April 2017 / Revised: 31 July 2017 / Accepted: 6 August 2017 / Published online: 18 August 2017

Abstract The retinal structure of the booted eagle (*Aquila pennata)* was investigated using light and electron microscopy. Particular attention is paid to the main ultrastructural features of the receptor cells. This study reveals six distinct varieties of cones. Unequal double cones differ in shape, structure, and length and are comprised by principal long and accessory short members. Principal member contains a green oil droplet and accessory member contains a paraboloid and a pale green droplet. Four types of single cones are distinguished on the basis of their morphology and oil droplets: red, green, blue, and ultraviolet. Cones outnumber rods in all regions. Two types of horizontal cells and several morphological types of amacrine cells are abundant. A large number of bipolar cells are divided into long longitudinal rows by Müller cell processes, a prominent feature of this retina. These processes extend through the external limiting membrane to reach the ellipsoid region of the cones. Moreover, thick processes divide the inner nuclear and plexiform layers and surround the myelinated ganglion cell axons at fairly regular intervals. In the ganglion cell layer and optic nerve fibre layer, abundant oligodendrocytes are present, close to the myelinated axons. The morphological characteristics of this retina indicate that *A. pennata* have good colour discrimination, a complex visual processing to mediate contrast and motion and an elevated acuity in areas of high cell densities.

✉ Yolanda Segovia
Yolanda.segovia@ua.es

[1] Department of Biotechnology, University of Alicante, Apartado 99, 03080 Alicante, Spain

Keywords Raptor vision · Avian retina · Oil droplets · Photoreceptor ultrastructure

Introduction

The relationships between the sensory systems posed by particular environments and the information that organisms extract from them have long been reported (Walls 1942; Lythgoe 1979; Martin and Portugal 2011). In this sense, the retinal morphology is the result of natural selection, as the animal's interactions with the environment modify the retina to achieve particular tasks. Thus, the retinal morphology of a given species is not determined by its taxonomic classification but rather by the functional requirements imposed upon the visual system by ecological and ethological factors (Wagner 1990).

In recent years, there has been great interest in the visual system of birds, as vision plays an important role in prey detection and capture, social interactions, reproductive behaviour, and in navigating their surroundings (Hart 2001; Rahman et al. 2006, 2007a, b; Jones et al. 2007; Ruggeri et al. 2010; Dolan and Fernández-Juricic 2010; Martin 2012; El-Beltagy 2015; Wilby et al. 2015). In general, the avian eye is very large in comparison with other animals; in fact, they occupy a major portion of the skull and often weigh more than the brain. The large size of the avian eye in relation with the size of the skull permits the formation of a large retinal image, which is an important feature in improving visual acuity (Meyer 1977; Jones et al. 2007). Typically, the avian retina is relatively thick compared to most other vertebrates and possesses a range of specialisations, which are a consequence of sensory ecology and adaptation to the environment. These specialisations are reflected in many aspects of the retinal structure such as (1)

the retinal cell morphology and the presence of an efferent centrifugal system (Cowan and Powell 1963; Hayes and Holden 1983; Fritzsch et al. 1990; Morgan et al. 1994; Fischer and Stell 1999; Uchiyama et al. 2004; Weller et al. 2009); (2) the existence of double cones which increase the area available for the absorption of light (Walls 1942; Gallego et al. 1975; Meyer 1977; Hart 2001; Rahman et al. 2007a, b; Jones et al. 2007), and act as a single functional unit used for motion perception (Maier and Bowmaker 1993; Vorobyev and Osorio 1998; Campenhausen and Kirschfeld 1998); (3) the presence in many cones of brightly coloured or colourless oil droplets, which reduce chromatic aberration and improve colour discrimination (Walls and Judd 1933; Walls 1942; Meyer 1977; Young and Martin 1984; Hart 2001; Vorobyev 2003; Hart and Vorobyev 2005; Wilby et al. 2015), protect against harmful ultraviolet radiation (Kirschfeld 1982; Hart 2001; Rahman et al. 2007a, b), enhance photon capture (Young and Martin 1984; Hart 2001), and detect the earth's magnetic field (Edmonds 1996; Hart 2001); (4) the existence of glycogen deposits (hyperboloids and paraboloids) in rod and cone myoids, which has been suggested as a possible adaptation for improving of visual acuity and as an energy sources for visual cell metabolism (Meyer 1977; Braekevelt 1993a, b); (5) the presence of diverse areas of higher visual acuity (visual streak, and single or double *foveae*) with an increased density of receptor cells and other neurons (Ehrlich 1981; Budnik et al. 1984; Ikushima et al. 1986; Naito and Chen 2004; Rahman et al. 2006, 2007a, b); (6) the existence of violet and ultraviolet-sensitive cones involved in foraging, signalling, and avian mate choice (Cuthill et al. 2000); and (7) the presence of the pecten oculi, whose main function is the nutrition of the inner layers of the avascular avian retina (Meyer 1977).

In this study, we examine the ultrastructure of the retina of the booted eagle (*Aquila pennata*). The booted eagle is a member of the Accipitridae family (order Accipitriformes) which inhabits forests, often in hilly countryside with some open areas of Africa, Asia, and Europe. On the Iberian Peninsula, it can be found in central and western regions, where unlike other raptors, populations appear to be remaining stable or increasing slightly. *Aquila pennata* is a medium-sized diurnal raptor (42–51 cm) with a wingspan of 110–135 cm. It may have two different plumage coloration phases, clear and dark, independently of the sex and the age of the bird. It is fundamentally a migratory bird, although in recent years, sedentary behaviour has been observed. It feeds mainly on medium-sized birds and rabbits, although it also captures some reptiles and large insects, depending on the abundance and accessibility of prey (http://www.seo.org/).

Two basic hunting techniques have been observed for the booted eagle: in open areas, it attacks prey obliquely, and in forests, it launches quickly into its prey. As in other predatory birds, vision is essential to its survival. The present study has the following aims (1) to describe the histological and ultrastructural architecture of the retina of the booted eagle retina, (2) to understand the morphology of the retina and its relationship with the lifestyle of the bird, and (3) to acquire further information data about the vision of predatory birds.

Materials and methods

Experimental animal and tissue preservation

For this study, an adult female booted eagle, *A. pennata*, was collected from the Santa Faz Wildlife Recovery Centre (Alicante) and euthanised by means of an intravenous overdose of sodium pentobarbital (Eutanax®) according to the European Union and the Spanish government regulations and standards for reasons not connected with this study. Both eyes were enucleated and hemisected carefully under normal room light. The retinas were removed and cut into four quadrants (nasal dorsal, nasal ventral, temporal dorsal, and temporal ventral) with the help of pecten positioning.

As tissue processing for electron microscopy destroys the oil droplet colour, which is a good marker of cone type (Kolb and Jones 1982), left eye was study in fresh. After isolation, the left cup eye was placed in 0.9% saline solution until the pigment epithelium detached from the retina. Quadrants of the left eye (nasal dorsal, nasal ventral, temporal dorsal, and temporal ventral) were placed on a gelatinised slide and rapidly examined under the microscope to observe that oil droplets Leica DMRB equipped with a Lumenera's INFINITY microscopy camera. Areas where oil droplets were visible were microphotographed at 40× magnification to associate a particular type of oil droplet with each of the cone classes.

Preparation for electron microscopy

Right eye was quickly dissected after collecting and the anterior portion including cornea, lens, and iris was cut away. After elimination of vitreous humor, the retina was excised from the eyecup and fixed immersed in the fixative (1% paraformaldehyde, 1.6% glutaraldehyde, 0.15 mm $CaCl_2$ in 0.1 M phosphate buffer, and pH 7.4) for 2 h and then at 4 °C overnight as described by Segovia et al. (2016). Small pieces from various regions were post-fixed in 2% OsO_4 in 0.1 M phosphate buffer for 1 h, pH 7.4 and then dehydrated in ascending series of ethanol, cleared in propylene oxide, and flat-embedded in Epon 812 epoxy resin. Blocks were oriented and semithin radial sections of

1.0 μm from each retinal quadrant were cut serially with a glass knife on a Leica LKB-III ultramicrotome. Sections were mounted on gelatinised slides, stained with 0.5% toluidine blue, and examined under a Leica DMRB light microscope. Photomicrographs of several sections (2–4) were taken with a Lumenera Infinity microscope camera. Ultrathin sections were cut with a diamond knife and double-contrasted with uranyl acetate and lead citrate and examined under a JEOL JEM-1400 Plus transmission electron microscope equipped with a Gatan Orius digital camera for image taking.

Photoreceptors can be differentiated under electron microscopy on the basis of outer segment shape, oil droplet, mitochondrial morphology, presence of paraboloid, nuclei position, and cytoplasm electron density.

Measurements of retinal layers

Measurements of the thickness of the entire retina and of each retinal layer were determined every 10 μm across 0.5 mm of each sample and averaged. From a collection of TEM electron micrographs, measurements of the lengths and diameters of outer and inner photoreceptor segments were made. Averaging counts were made from cells of ten grids selected haphazardly. Only cells cut centrally through their paraboloid, ellipsoid, and outer segments were chosen for measurements.

Results

General description

As in all vertebrate retinas, the retina of the booted eagle is organised into ten well-defined layers. Under light microscopy, differences in thickness can be noted in different regions of the retina as well as in number and cellular subtypes: there are noticeable variations in the number and type of photoreceptors, number of bipolar cells, and size and type of amacrine and ganglion cells. The photoreceptor layer (PL) is composed primarily of cones which differ in number and type. Rods are easily recognizable by the largest and widest outer segments and by being free of oil droplets (Fig. 1a). The morphology of the inner nuclear layer (INL), inner plexiform layer (IPL), ganglion cell layer (GCL), and optic nerve fibre layer (NFL) shows considerable differences (Fig. 1a, b). The relative thickness of the outer retina (including the pigment epithelium) compared to the inner retina is 1:2, except in the *areas,* where the inner retina is larger. Figure 1b shows a temporal *area* associated with an increase of cell density in all cell layers, making the retina thicker than elsewhere.

Whole mount retinas from fresh preparations observed under light microscopy make it possible to distinguish oil droplets of different colours located on different levels: green, red, yellow, pale green, and colourless (Fig. 2a). Green oil droplets are the largest (4.12 ± 0.61 μm) and are located at the most scleral level into the principal member of double cones. They are named P-type oil droplet (P-type). The accessory member of the double cones has a pale green droplet (A-type droplet) when observed in fresh retinas (Fig. 2a), which is intensely stained with tolouidine blue and electron dense (0.4–2 μm) under electron microscopy. In some cases, a diffuse aggregation of this droplet is observed in the ellipsoid region. Yellow (Y-type oil droplet) and red (R-type oil droplet) oil droplets (3.3 ± 0.24 and 3.8 ± 0.35 μm, respectively) are observed at the same level of focus and vitread to P-type oil droplets. Finally, colourless (2.6 ± 0.17 μm) droplets (C-type oil droplets) are located in the most vitread focus (Fig. 2a).

According to others' reports (Bowmaker et al. 1997; Hart 2001; Hart and Vorobyev 2005), who have established a relationship between the type of oil droplet and the spectral sensitivity of the different photoreceptor cones in avian retinas, red oil droplets are located in red single cones and green oil droplets in the principal members of double cones. Both cones have visual pigments that absorb light at long wavelengths (LWS 543–571 nm). The yellow oil droplet corresponds to the green single cone that absorbs light at medium wavelengths (MWS 497–510 nm). Colourless droplets occur in single blue and ultraviolet/violet cones with short wavelengths of maximum absorption (SWS 430–463 nm). Figure 2b shows the different photoreceptor cell types.

Electron microscopy

Retinal pigment epithelium

The RPE of the booted eagle consists of a single layer of cuboidal cells that lies in the Bruch's membrane which separates the pigment epithelial cell from the vascular choroidal tissue. The RPE cells measure about 9.13 ± 1.21 μm in height and display numerous infoldings on their base (Fig. 3a, b), penetrating to a depth of about 1.3 ± 0.23 μm and usually quite uniform in length within each cell. In the apical border of the cell, numerous finger-like processes (19.8 ± 1.8 μm) project from the RPE cell body towards the retina, interdigitating with the outer and inner segments of the photoreceptor cells; melanin granules are observed close to the ellipsoid. The length of the processes differs in different regions until they disappear into the peripheral retina. The lateral margins of cells, which are relatively smooth, are joined laterally by a series of tight junctions and *zonula adherens* (Fig. 3b).

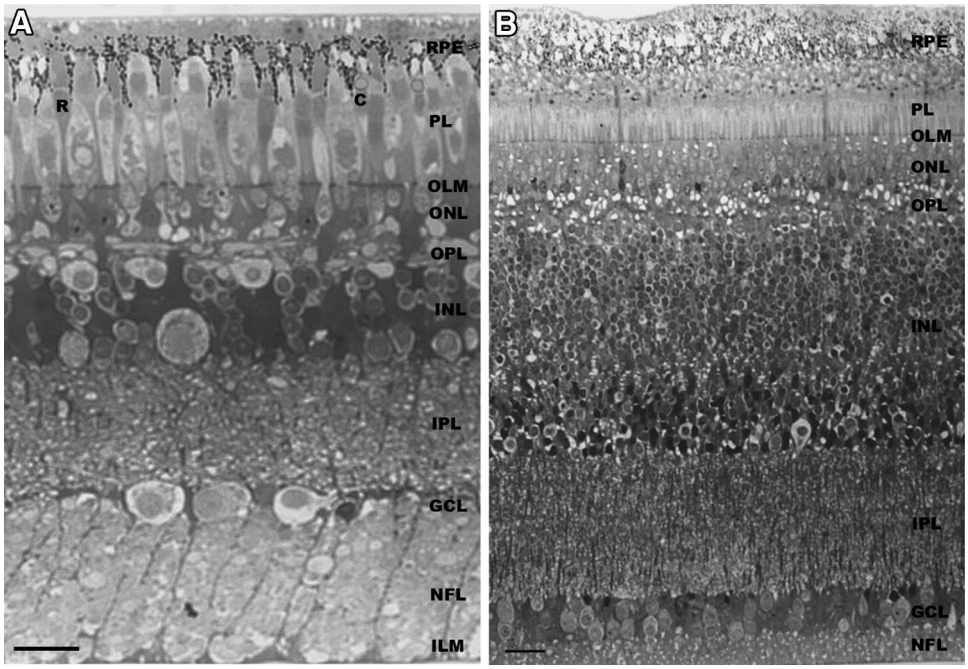

Fig. 1 Light micrographs of 1 µm semithin sections stained with toluidine blue from different regions of the booted eagle retina. **a** Peripherical region. **b** Central region (*area*). Differences are observed in the thickness of all layers and the abundance of cell types. Retinal pigment epithelium (*RPE*), photoreceptor layer (*PL*), cone (*C*), rod (*R*), outer limiting membrane (*OLM*), outer nuclear layer (*ONL*), outer plexiform layer (*OPL*), inner nuclear layer (*INL*), inner plexiform layer (*IPL*), ganglion cell layer (*GCL*), optic nerve fibre layer (*NFL*), inner limiting membrane (*ILM*). *Scale bar* 20 µm

The vesicular nucleus of these cells is located in the basal region of the cell (Fig. 3a). The cytoplasm is filled with vesicles and tubular smooth endoplasmic reticulum (SER), the most abundant cell organelle apart from the basal infoldings. Rough endoplasmic reticulum (RER) is not abundant, but is noted as isolated profiles. The basally located mitochondria are numerous and the majority are round and oval in profile (Fig. 3a, b).

An abundant number of melanin granules are located within the apical processes of the cells (Fig. 3a, b). Whereas in the middle zone of the cell, the granules are round, and in the apical processes, the melanosomes are arranged parallel to the length of the processes. We observed lysosome-like bodies and outer segment phagosomes. Myeloid bodies, lenticular-shaped accumulations of smooth membranes, were also noted in the middle region of the RPE cell (Fig. 3b).

Photoreceptor layer

The photoreceptor layer consists of three types of visual cells: rods, double cones, and single cones, with a clear predominance of cones over rods. The presence of different types of cones depends on the region of the retina.

Rod photoreceptors

Rod photoreceptors, which are slender and less numerous than cone photoreceptors, have a large and cylindrical outer segment measuring 19.8 ± 0.49 µm in length and 2.87 ± 0.47 µm in width (Fig. 4a). The rod outer segments are surrounded by the apical processes of the RPE cells and are joined with their inner segments by a connecting cilium that displays a thick striated filament, known as the ciliary rootlet (Fig. 4b). This structure extends from the proximal ends of the basal bodies towards the ellipsoid end of the cells and is also present in cones.

The diameter of the inner segments of the rods is about 3.67 ± 0.51 µm, although a narrowed region can gradually be observed over the myoid. Immediately below the connecting cilium, within the ellipsoid region, the rod photoreceptors display an accumulation of electron-dense mitochondria, which are orientated along the long axis of the cell (Fig. 4c). No oil droplet is observed, but a dense accumulation of glycogen granules is noted residing in the myoid region, the so-called hyperboloid (Fig. 4c). Normally, the entire cytoplasmic area and rod nuclei are more electron dense than in cones. The myoid, which is often difficult to locate amongst the cone photoreceptors, is a long and slender part of the cell, reaching from the ellipsoid to the outer limiting membrane (OLM). Near the OLM, polysomes and Golgi zones are observed, as are RER profiles.

The nuclei of the rod photoreceptors are located vitread in the outer nuclear layer (ONL) close to the outer plexiform layer (OPL). From the nuclei, in some cases, short and thick processes descend obliquely and terminate horizontally through the distal zone of the OPL (Fig. 4d). Rod synaptic terminals, or spherules, have numerous synaptic vesicles which differ from those of cones in electron density and concentration. The spherules contain several

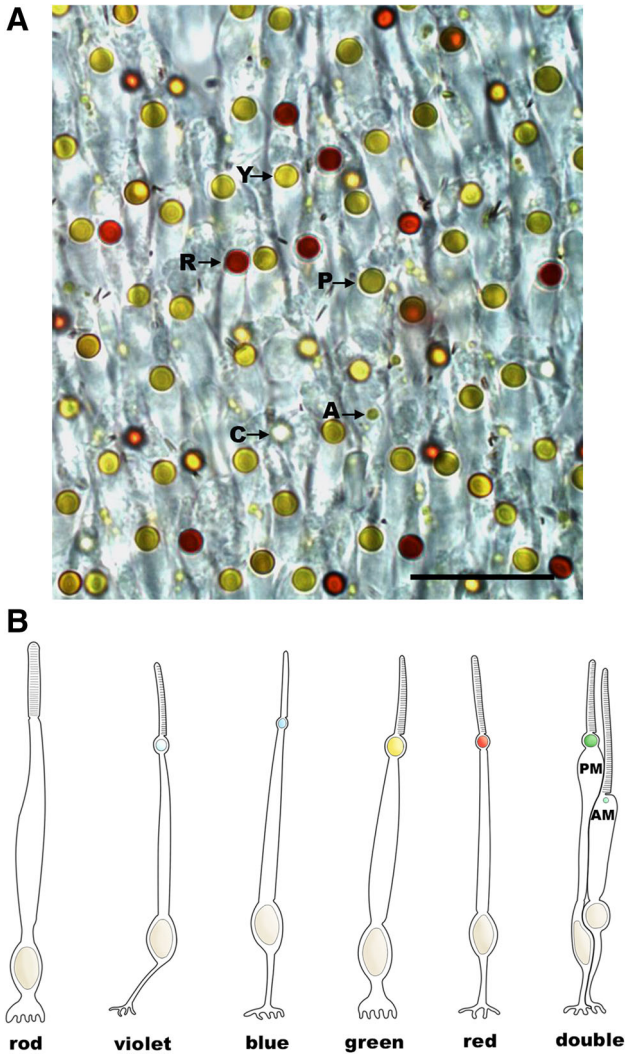

Fig. 2 **a** Micrographs showing the topography of coloured oil droplets in a whole mount under bright-field illumination. *R*, *Y*, *P*, *A*, *C* correspond to R-, Y-, P-, A-, and C-type oil droplets. *Scale bar* 20 µm. **b** Diagram of the photoreceptor cell types

synaptic ribbons approximately 0.45 ± 0.16 µm in length (Fig. 4e).

Double cones

The double cones, the dominant photoreceptor in *A. pennata*, are characterised by the close apposition of their two members. They consist of a longer principal member and a smaller accessory cone with a paraboloid. They touch one another except in the outer segments, which are separated, so that the two members are closely packed without any interposition of pigment epithelium or Müller cell processes (Fig. 5a). The inner segment of the principal member has its widest portion at the scleral end and the inner segment of the accessory member is widest at the vitreal end. The principal member displays a large green oil droplet which measures 4.12 ± 0.61 µm in diameter. A minute green pale droplet is observed in the accessory member (Fig. 5a).

Underneath the outer segment of each type of cone, there is an accumulation of densely packed mitochondria. The ellipsoidal mitochondria of the principal member are angular, wider, and denser than those of the accessory member, which have clear, round mitochondria. The inner segment of the principal member is also similar in all major features to the inner segment of a single cone, except that the myoid of the former is much longer and thinner. The pear-shaped inner segment of the accessory member contains the so-called paraboloid, located at the vitreal end of the ellipsoid, with abundant glycogen granules associated with several profiles of both types of endoplasmic reticulum (Fig. 5a, c, d).

The nuclei of double cones are ovoid and display a similar size. Both nuclei display a vesicular chromatin and lie in the most scleral level of the ONL; however, the nuclei of the principal members have more heterochromatin clumps. A feature of double cones is that the nucleus of the accessory member protrudes beyond the OLM (Fig. 5d, e). A narrow axon ends in pedicles at the most distal level of the OPL.

Red and green single cones

Ultrastructurally, these single cones are recognized by the oil droplets which in single reds are paler and smaller than dark yellow oil droplets. In the *area*, these cones are coupled, having their oil droplets joined (Fig. 5b).

They are typically elongated and the entire cytoplasmic area is lightly stained. The ellipsoid is densely packed with electron-dense mitochondria and no paraboloid is observed. The inner segment displays numerous polysomes and a characteristic spiral RER profile, which can be observed in Fig. 5c. The nuclei of single cones are vesicular and are located in the middle part of the ONL. The synaptic pedicles, which are indistinguishable from each other, are pyramidal or pear-shaped. Their base displays several invaginations with 2–7 synaptic ribbons which measure 0.35 ± 0.18 µm and are related to three invaginated processes (triad), two lateral elements probably of horizontal cells and a central element probably of a bipolar cell (Fig. 5e). In addition, several convectional synaptic sites can be observed in both photoreceptor terminals.

Blue and ultraviolet/violet single cones

The blue single cone is the slenderest one. The ellipsoid is darker and slimmer. The C-type oil droplet is located below the red and yellow ones. The axon is long and ends

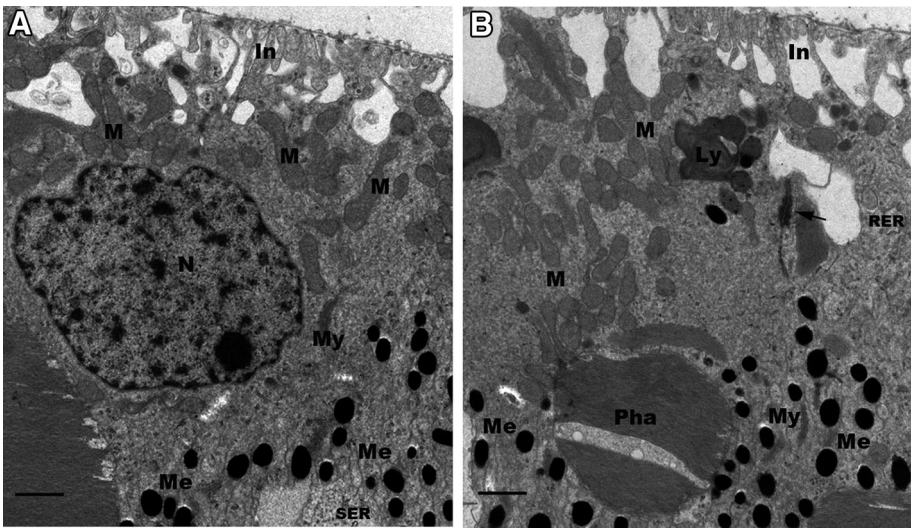

Fig. 3 **a** Electron micrograhs of RPE show the basal infoldings (*In*), the vesicular nuclei (*N*), the basally located mitochondrion (*M*), smooth endoplasmic reticulum (*SER*), lysosomes (*Ly*), myeloid bodies (*My*), and melanin granules located apically (*Me*). *Bar* 1 μm. **b** Electron micrographs of RPE showing a large phagosome (*Pha*), isolated profiles of rough endoplasmic reticulum (*RER*), and a *zonula adherens* (*arrow*) in the lateral margin. *Scale bar* 1 μm

in a pedicle which is between other synaptic terminals (Fig. 5f).

The ultraviolet/violet cone is smaller than the other single cones and contains a C-type oil droplet. The ellipsoid shows densely packed mitochondria. This cone differs from other single cones in the orientation and termination of its axons. This process is long and curved, becoming almost horizontal in the outer plexiform layer. Moreover, the pedicles reach to the most proximal level of this plexiform layer.

Outer limiting membrane

This "membrane" is composed of attachment zones between Müller cells or between Müller cells and receptor cells. Dark and extended Müller cell processes and *zonulae adherens* with photoreceptor cells are very evident. Typically, electron-dense mitochondria have accumulated close to the OLM (Fig. 5d). Glial elements completely separate the receptors from each other with the exception of the two members of the double cones.

Outer nuclear layer

The ONL displays photoreceptor nuclei arranged in several rows. This layer is 17.7 ± 4.8 μm thick and is quite uniform across the retina; however, in the *area*, it attains a thickness of 28.6 μm.

Outer plexiform layer

The thickness of the OPL is quite uniform in the different regions of the retina (11.33 ± 1.95 μm in thick), and under electron microscopy reveals an extreme complexity (Fig. 6a). Three distinct zones can be observed: (1) the outer zone, formed by pedicles, spherules, and the dendrites of bipolar and horizontal cells; (2) the middle zone, consisting of small dendrites of bipolar cells and horizontal cells; and (3) the inner zone, composed of the horizontally displaced axons of horizontal cells.

Inner nuclear layer

The INL is formed of different cell types including horizontal, bipolar, amacrine, and Müller cells (Fig. 6b). This layer is 52.5 ± 17.48 μm thick in the central retina and 19.88 ± 0.17 μm in the peripheral one, although its thickest point is in the *area*, where it reaches 120 μm. In the outer zone, near the OPL, we can identify, presumably, two types of horizontal cells, differentiated by cytoplasm size: (1) a large cell with a large nucleus and clear cytoplasm, with a diameter of 10.55 ± 2.23 μm (Fig. 6b) and (2) a small cell, of about 5.26 ± 0.37 μm in diameter, with a large apical process (13.28 ± 0.66 μm) rising from the inner zone of the OPL (Fig. 6a). Both types send dendrites to the OPL, where they establish synapses with the photoreceptor terminals.

Bipolar cells, located between the horizontal and amacrine cells, characteristically form longitudinal rows, which vary in number depending on the region (from 2 to 3 cells in the peripheral regions to 20–22 cells in the *area*), and are separated by Müller cell cytoplasm (Fig. 6b). The cell body is either round or oval in shape (6 ± 1.13 μm in diameter) and has a round nucleus. Some of these cells also contain apical dendrites with several cytoskeleton elements and SER profiles can also be noted in some of these cells, spreading towards the OPL, where they establish synapsis.

Presumed amacrine cells are distinguished from bipolar cells by their size, their location, and the arrangement of their cytoplasm (Fig. 6b). These cells are located in the

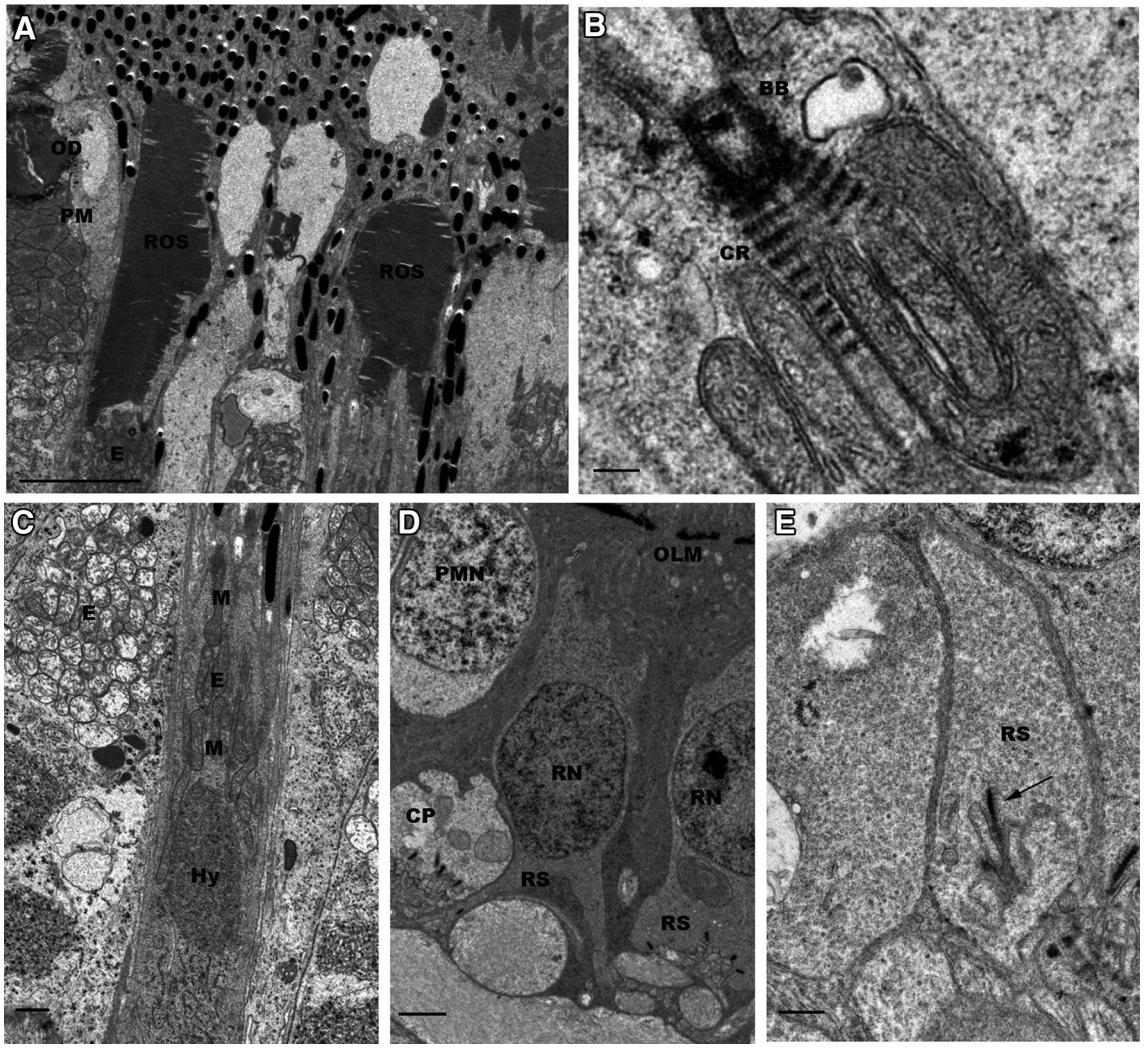

Fig. 4 **a** Electron micrograph of a rod photoreceptor showing the outer segment (*ROS*) and ellipsoid (*E*) with electron-dense mitochondria (*M*). The principal member of a double cone (*PM*) with a large oil droplet (*OD*) is observed. *Bar* 2 µm. **b** Electron micrograph of the ciliary rootlet (*CR*), which originates from the basal bodies (*BB*) below the connecting cilium and extends longitudinally. *Bar* 0.5 µm. **c** Electron micrograph of a rod photoreceptor, showing the hyperboloid (*Hy*) and ellipsoid (*E*). The ellipsoid (*E*) of a principal member is also observed. *Bar* 1 µm. **d** Electron micrograph of outer nuclear layer close to the outer limiting membrane (*OLM*) illustrates a rod nucleus (*RN*) and a principal member nucleus (*PMN*). Cone pedicles (*CP*) and a rod spherule (*RS*) are also indicated. *Bar* 2 µm. **e** Electron micrograph of a rod spherule (*RS*) in which the synaptic ribbon (*arrow*) is evident. *Scale bar* 0.5 µm

most inner zone of the INL. The cell bodies display a big variation in diameter, are round to oval in shape, and have abundant cytoplasm, more than the bipolar cells. The perikaryon contains the usual neuronal cytoplasmic organelles and a round dark nucleus with disperse chromatin granules. The descendant processes of these cells reach the IPL, where they establish synapses with bipolar and ganglion cells.

The Müller cells are the most important glial cells of the retina. These cells extend radially forming the OLM and the ILM, and have a fusiform cell body with an oval nucleus located in the middle part of the INL (Fig. 6b). Their cytoplasm is very dark and their processes penetrate between all the neurons, forming a complex structure. In the INL, these processes separate the rest of the cells into rows of several cells.

Inner plexiform layer

The IPL, which has a thickness of 44.82 ± 7.16 µm in the central retina and 37.38 ± 3.7 µm in the peripheral retina, is a region in which three different types of neurons (bipolar, amacrine, and ganglion cells) interact through their synaptic processes, forming an intricate network with the Müller cell processes.

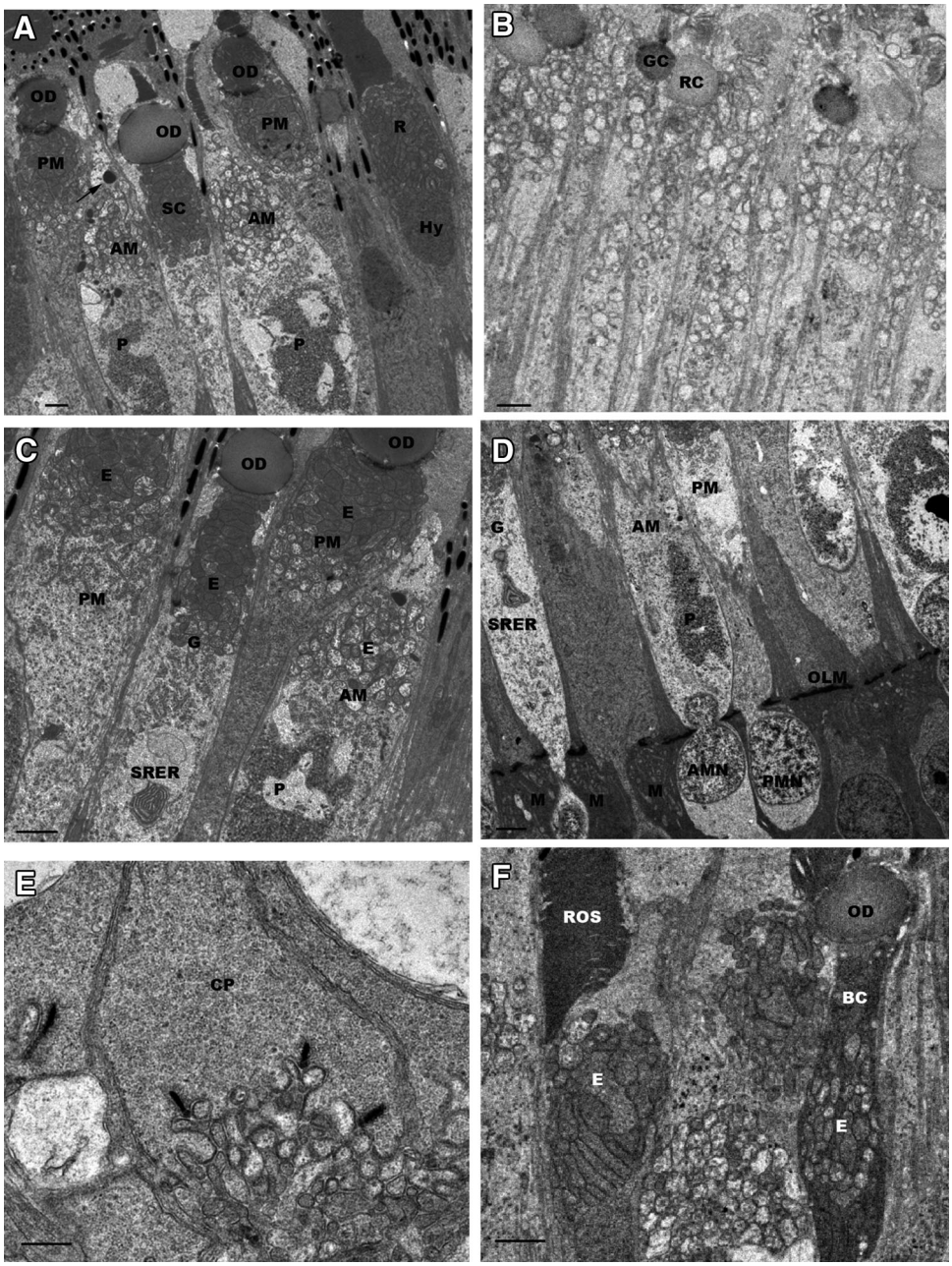

Fig. 5 **a** Electron micrograph of cone photoreceptors showing two double cones formed by the principal member (*PM*) and the accessory member (*AM*) which shows a paraboloid (*P*). *Arrow* indicates the minute droplet of the AM. A single cone (*SC*) with a large oil droplet (*OD*) is observed. *Bar* 2 µm. **b** Electron micrograph of cone photoreceptors in the *area* shows red and green single cones (*R* and *G*, respectively). Both present oil droplets which differ in electron-density. *Bar* 2 µm. **c** Electron micrograph of cone photoreceptors showing the principal (*PM*) and accessory member (*AM*) of a double cone as well as a green single cone (*G*) with a characteristic rough spiral endoplasmic reticulum (*SRER*). Oil droplets (*OD*), ellipsoids (*E*), and the paraboloid (*P*) of the accessory member are also seen. *Bar* 2 µm. **d** Electron micrograph of cone photoreceptors taken near the outer limiting membrane (*OLM*). This micrograph shows the principal (*PM*) and the accessory member (*AM*) of a double cone, a green cone (*G*) with a rough spiral endoplasmic reticulum (*SRER*), the nucleus of the accessory member (*AMN*) which protrudes beyond the OLM, the nucleus of the principal member (*PMN*), and an accumulation of electron-dense mitochondria (*M*) close to the OLM into the Müller cells. *Bar* 2 µm. **e** Electron micrograph from transverse section of the retina showing the ultrastructure of a cone pedicle (*CP*) with three synaptic ribbons. *Bar* 0.5 µm. **f** Electron micrograph showing in the left the outer segment (*ROS*) and ellipsoid (*E*) of a rod photoreceptor and in the right a blue single cone (*BC*), in which the oil droplet (*OD*) and the dark ellipsoid (*E*) are indicated. *Scale bar* 2 µm

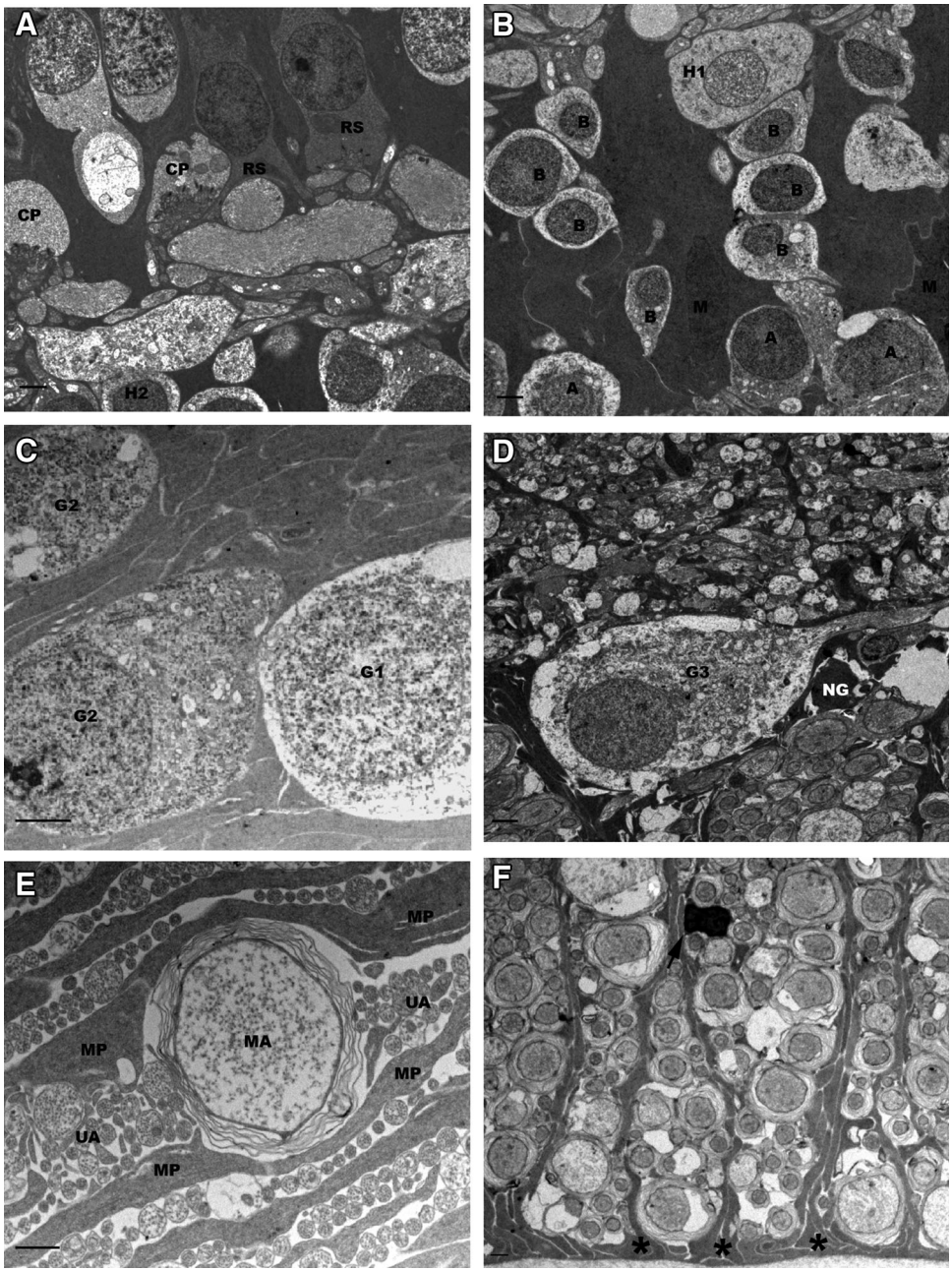

Fig. 6 **a** Electron micrograph taken near the OPL which shows cone synaptic pedicles (*CP*) and rod synaptic spherule (*RS*). A presumed small horizontal cell with a big apical process is also indicated (*H2*). *Bar* 2 µm. **b** Electron micrograph of the INL showing horizontal (*H1*), bipolar (*B*), and amacrine cells (*A*) which are separated by the processes of Müller cells, whose nuclei (*M*) are present in the middle part of the INL. *Bar* 2 µm. **c** Electron micrograph of three middle-sized ganglion cells, one with clear cytoplasm and pale nucleus (*G1*) and two with dark cytoplasm (*G2*). *Bar* 2 µm. **d** Electron micrograph of a giant pyriform ganglion cell (*G3*) with clear cytoplasm and darkly round nucleus, and a small neuroglial cell (*NG*). *Bar* 2 µm. **e** Electron micrograph of the NFL showing bundles of unmyelinated axons (*UA*) and a big myelinated axon (*MA*) separated by the processes of Müller cells (*MP*). *Bar* 1 µm. **f** Electron micrograph of the NFL showing bundles of myelinated axons, the end feet of Müller cells (*asterisk*) forming the ILM. Note the presence of an oligodendrocyte (*arrow*). *Scale bar* 2 µm

Ganglion cell layer

The GCL consists of a single row of ganglion cells about 13.5 ± 3.34 µm thick in both the central and the peripheral retina. It is thickest in the *area* (about 26 µm) and there are 2–3 rows of ganglion cells.

In the peripheral retina, the size of ganglion cells varies greatly, forming a heterogeneous population of large- and medium-sized ganglion cells, whereas in the *area,* cell size is very uniform and a relatively homogeneous population of medium-sized cells is observed. We can identify three types of ganglion cells, differentiating them by their morphology: (1) a middle-sized cell, of about 8.12 ± 0.74 µm in diameter, oval in shape, with clear cytoplasm and a pale round nucleus (Fig. 6c); (2) a middle-sized pyriform cell, about 8.5 ± 1.37 µm in diameter, with dark cytoplasm and a prominent nucleolus (Fig. 6c); and (3) a giant pyriform cell, about 17.12 ± 3.46 µm in diameter, with clear cytoplasm, a round, dark nucleus and a prominent nucleolus (Fig. 6d). The cytoplasm of these cells shows the typical neuronal features: mitochondria, Golgi apparatus, and Nissl substance among others, and their axons run parallel to the inner surface of the retina forming the NFL.

In this layer, there are also abundant neuroglial cells, which are smaller than the ganglion cells and have sparse dark cytoplasm with a small, round dark nucleus (Fig. 6d). These cells cannot be distinguished without histological markers, but as they are found near myelinated ganglion cell axons, may be oligodendrocytes (Fig. 6f).

Optic nerve fibre layer

The thickness of the NFL is not uniform along the retina. In this layer, we can distinguish longitudinal bundles of unmyelinated and thinly myelinated ganglion cell axons, and are separated by processes and the end feet of Müller cells, which form the inner limiting membrane (ILM) (Fig. 6e, f).

Discussion

Although there have been several studies on the visual system of raptors in the past, not much information is available. Essentially, ethical reasons and the legal protection of bird of prey meant that research material was scarce, and also, material for histological studies is very limited. As the raptor retina represents a huge gap in our knowledge, this study, though based on just one sample, is necessary and interesting as a starting point for future research and for comparison with other avian raptors or bird species. More samples would be necessary to perform microspectrophotometry and quantitative analyses of cells and their relative proportions and topographical distribution throughout the retina.

Retinal pigment epithelium layer

The pigment epithelium is formed by a single layer of cuboidal cells located between the rod and cone photoreceptors and the vascular bed of the choriocapillaris which are rich in organelles and inclusions. The outer border of the epithelial cells is highly infolded and presents numerous mitochondria, as reported for other raptor species (Braekevelt 1992; Braekevelt and Thorlakson 1993; Braekevelt et al. 1996a). This observation is indicative of the high transport rate of these cells. The vitreal surface displays numerous processes which interdigitate with photoreceptor outer and inner segments and are filled with abundant melanosomes. Unlike the central retina, in the peripheral and area regions, where cones are larger and slenderer than in the central retina, and they are highly packed, melanosomes are only found surrounding outer segments. It has been suggested that melanosomes in the apical processes of these cells contribute to the effective light absorption, preventing scattering and the subsequent reduction of visual acuity (Walls 1942). This is thought to be done by photomechanical movements, which are rapid and extensive in all birds (Meyer 1977). However, studies under dark–light are required to confirm this in the booted eagle.

Other important functions include providing structural support for the long outer segments of the photoreceptors (El-Beltagy 2015), orientating them properly to get the light in the proper direction and supplying internal support to the retina by joining together the pigment epithelium and the photoreceptors (Braekevelt and Thorlakson 1993). They are also involved in the phagocytosis of the oldest membranous discs of the outer segment (Young and Bok 1979); vitamin A (retinol) uptake, processing, transport, and release; building up the blood–retina barrier; and transporting blood to the retina and back (Schraermeyer and Heimann 1999). In addition, the RPE melanosomes have been shown to catalyse free radical activity, especially when illuminated with visible or ultraviolet light (Dontsov et al. 1999).

Photoreceptors, oil droplets, and colour vision

As in other diurnal birds, in the booted eagle cone, photoreceptors outnumber rods in all regions of the retina (Hart 2001; Jones et al. 2007; Rahman et al. 2007a, b). In general, the response of rods to light is slower but more sensitive than the response of cones in the same retina and they are capable of functioning at very low light intensities, such as twilight levels (Yau 1994; Lamb 2009). Nevertheless, the preponderance of cones over rods in diurnal vertebrates allows the retina to respond rapidly to incoming light, as well as giving it the ability to respond to an enormous range of light intensities (Lamb 2009). This supports the abundance of several types of cones in the booted eagle, suggesting that diurnal and colour vision may be important in predation activities. The only raptor in which a microspectrophotometric analysis of cones has been investigated is *Strix aluco*, a trichromatic nocturnal raptor with peak wavelengths of spectral sensitivity of 463, 503, and 555 nm in the different cone types (Bowmaker and Martin 1978). However, as the booted eagle is a diurnal raptor, it is reasonable to expect it to have multiple spectral classes of cones and more complex colour vision. According to light microscopy literature on avian retina (Hart 2001; Jones et al. 2007; Rahman et al. 2007a, b), the booted eagle has a single class of rods, a single type of double cones and several types of single cones, which are characterised by the presence of oil droplets located at the distal end of their inner segments. We distinguished five types of oil droplets: red, yellow, colourless, green, and pale green. Bowmaker et al. (1997), Hart and Vorobyev (2005) and Hart et al. (2006) established a relationship

between spectral cone visual pigments and oil droplets, making it possible to classify them. Red oil droplets have been associated with long-wave-sensitive cone pigment (LWS or red), yellow droplets with medium-wave-sensitive cone pigment (MWS or green), colourless droplets with a short-wave-sensitive cone pigment (SWS or blue), and transparent with ultraviolet/violet cone pigment (UVS/UV). We could not distinguish between colourless and transparent oil droplets under bright-field microscopy. Moreover, Bowmaker et al. (1997) and Hart et al. (1998) have described an oil droplet in the accessory member which contains a low concentration of carotenoid pigment and an absorption spectrum between 420 and 480 nm, lower than found in other oil droplets. In this way, a characteristic feature of the booted eagle retina is the presence of a droplet in the accessory member of the double cones, which is electron dense under electron microscopy and pale green under light microscopy. Occasionally, this droplet is fragmented around the ellipsoid. Additional research is necessary to identify the chemical composition of this droplet and its absorption spectrum before assigning it any functional hypothesis.

Coloured oil droplets are also present in lungfishes, turtles, and diurnal lizards (Walls 1942; Gallego et al. 1975; Kolb and Jones 1982; Khattab et al. 2004). The colouring of oil droplets depends not only on the spectral identity of the cone (Hart et al. 2006), but also on the region of the retina in which it is found and the living habits of the different species (Meyer 1977). Thus, they tend to be brightly coloured in diurnal species, whereas in nocturnal species, they appear colourless or pale yellow (Walls 1942; Meyer 1977; Hart 2001). Changes in oil droplet colour are thought to be a result of genetic selection for improving cone sensitivity under different light conditions. It has also been suggested that they could serve as low-pass filters, exposing the photopigment only to light that has a longer wavelength (Beason and Loew 2008), thus reducing the overlap in the sensitivity of adjacent cones and increasing the number of colours that birds can distinguish (Hart 2001; Vorobyev 2003). Other theories include the reduction of chromatic aberration and enhancement of contrast (Walls 1942), protection against harmful ultraviolet radiation (Kirschfeld 1982) or enhancing photon capture (Young and Martin 1984).

The proportion of these oil droplets also varies depending on the species and the different regions of the retina. This variation reflects different colour discrimination capabilities as well as differences in visual ecology (Muntz 1972; Goldsmith et al. 1984; Hart 2001). Whereas in ground-feeding birds, such as the blackbird and the starling, double cones have been observed only in the dorsal half of the retina (Hart et al. 2006), and in booted eagle retina, green oil droplets located at the principal member of double cones are the most abundant droplets across the retina. These cones have been implicated in movement detection rather than of wavelength discrimination (Maier and Bowmaker 1993; Vorobyev and Osorio 1998; Campenhausen and Kirschfeld 1998). In bootle eagle, movement detection is very important when gliding, to sight prey and would mean a great advantage in the feeding habits of the booted eagle. Moreover, the presence of all types of single cones in the area confers excellent colour discrimination. In this sense, it has been suggested that these cones (with red and yellow oil droplets, respectively) would be helpful in distinguishing between different types of foliage (Bowmaker 1977; Lythgoe 1979).

As in all vertebrates, there is an accumulation of mitochondria (ellipsoid) at the apex of the inner segments of the different photoreceptors, differing in distribution and orientation among each photoreceptor. It has been suggested that in nocturnal animals, this region may act as a convex lens, condensing the light on the outer segment and enhancing visual ability; however, this is unnecessary in diurnal animals (Khattab et al. 2004; El-Beltagy 2015). In the booted eagle, the ellipsoid is not a bulky region and the possibility of it acting as a lens is improbable.

Another peculiar structure inside the inner segments of the photoreceptors of the booted eagle is the presence of glycogen deposits in rods and the accessory member of the double cones. Although these deposits are not observed in the photoreceptors of nocturnal raptors such as the great horned owl and the barred owl, these species have glycogen granules widely dispersed throughout the inner segment of their cones, forming a diffuse type of paraboloid (Braekevelt 1993b, 1996b). The variation in different species and the function of these deposits are not clear, although, however, they are thought to be a possible adaptation to improve visual acuity, as they have a high refraction index, enabling them to concentrate light onto the outer segments (Meyer 1977). It has also been suggested that they could act as energy storage for visual requirements, substituting for Müller cell glycogen, which is much reduced in the avascular avian retina (Uga and Smelser 1973; Meyer 1977).

Inner retina and intraretinal variations

Inner nuclear layer and inner plexiform layer

The thickness of the INL and IPL suggests that this retina presents a high degree complexity in processing and neural interactions. We observed, presumably, two types of horizontal cells close to the outer plexiform layer: one cell with a large nucleus and sparse cytoplasm, and another with a large and pale cytoplasm with a large apical process, located close to the OPL. These cells may correspond to

stellate and brush-shaped horizontal cells, as described by Cajal (Rodieck 1973).

Bipolar cells constitute the bulk of INL, so that up to 22 rows of cell can be observed in the area. Amacrine cells display great morphological diversity. Nalbach et al. (1993) have reported a high number of amacrine cells in birds, possibly higher than in other vertebrates. They have also observed regional variations in amacrine cell density in the pigeon retina, with large numbers of amacrine cells in the dorso-temporal quadrant. This might explain the predominance of complex responses and directional selectivity in avian retinal ganglion cells compared to those in mammals.

Ganglion cell layer and optic nerve fibre layer

Ganglion cell density in the retina of the booted eagle differs in peripheral and central regions and the size of cell soma is inversely proportional to cell density. Specifically, one of the studied regions of the booted eagle central retina presents the maximum thickness in all of its layers, compatible with the *area* observed in other raptors (Jones et al. 2007) and with the horizontal streak reported in Falconiforms (Bravo and Pettigrew 1981). Because of the high amount of photoreceptors, ganglion cells, and other cells in the inner nuclear layer, this region enables the animal to scan a broad horizon without the distinctive eye movements needed for scanning with an area centralis and to perceive movements at a lower threshold (Tancred 1981).

In addition to excellent panoramic sight, many raptors, such as eagles, hawks, and falcons, which most need accurate distance vision, have one fovea located in the temporal retina and another located centrally. It has been suggested that the central fovea serves primarily as the lateral monocular visual field and for fixation of distant objects, and the temporal fovea is dedicated primarily to binocular vision (Pettigrew 1978; Inzunza et al. 1991; Jones et al. 2007). The presence of these specialisations may explain the high visual acuity of birds: *Aquila audax* can see about 2.5 times better than humans, while the acuity of falcons is very similar to the highest acuity of humans (Reymond 1987; Hirsch 1982; Gaffney and Hodos 2003).

Using electron microscopy, we observed no fovea and further research is necessary to confirm their existence.

Glial cells

As in other avian retinas studied, Müller cells are the only astroglial cells observed in the retina of the booted eagle (Won et al. 2000). The thick processes of Müller cells are very prominent in the NFL, dividing the nerve fibre surrounding the myelinated ganglion cell axons (unlike those found in most mammalian species) at fairly regular intervals. Moreover, all nuclear layer cells are surrounded by Müller cells. Finally, as has recently been reported in other avian species (Won et al. 2000; Seo et al. 2001), the abundant presence of oligodendrocytes is a feature of this retina. In addition to their role in myelination, oligodendrocytes are also believed to play a trophic role (Seo et al. 2001).

Conclusions

Although further study is required to understand intraretinal cell variation, colour vision, and spatial resolution in the booted eagle, this paper offers interesting findings about the retina of this raptor. We have observed that the retina of the booted eagle is greatly specialised, and we highlight five aspects of its retinal morphology: (1) the relative thickness of the retina itself shows high degrees of diversity; (2) a high diversity of cones and a high degree of differentiation; (3) the different morphology and the presence of brightly coloured oil droplets result in at least six functional cone types and good colour discrimination; (4) the presence of specialised areas that may contribute to the relatively greater visual acuity of booted eagle compared to other birds; and (5) the relative thickness of the inner retina and the cellular diversity suggest a high degree of movement and contrast detection, control of sensitivity, and high resolution.

Acknowledgements This research was supported by the University of Alicante VIGROB-186 and UAUSTI16-06. We thank Drs. P. María-Mojica and A. Izquierdo of the Santa Faz Wildlife Recovery Centre for helping to obtain the samples used in this study and Vanessa Pinilla for technical support. The authors are indebted to Noemí Victory Fiol for the image, as presented in Fig. 2b. Sampling was authorized by the Regional Valencian Ministry of Agriculture, Natural Environment, Climate Change, and Rural Development.

References

Beason RC, Loew ER (2008) Visual pigment and oil droplet characteristics of the bobolink (*Dolichonyx oryzivorus*), a new world migratory bird. Vis Res 48(1):1–8

Bowmaker JK (1977) The visual pigments, oil droplets and spectral sensitivity of the pigeon. Vis Res 17(10):1129–1138

Bowmaker JK, Martin GR (1978) Visual pigments and colour vision in a nocturnal bird, *Strix aluco* (tawny owl). Vis Res 18(9):1125–1130

Bowmaker JK, Heath LA, Wilkie SE, Hunt DM (1997) Visual pigments and oil droplets from six classes of photoreceptor in the retinas of birds. Vis Res 37(16):2183–2194

Braekevelt CR (1992) Retinal pigment epithelial fine structure in the red-tailed hawk (*Buteo jamaicensis*). Anat Histol Embryol 21(1):48–56

Braekevelt CR (1993a) Retinal photoreceptor fine structure in the red-tailed hawk (*Buteo jamaicensis*). Anat Histol Embryol 22(3):222–232

Braekevelt CR (1993b) Fine structure of the retinal photoreceptors of the great horned owl (*Bubo virginianus*). Histol Histopathol 8(1):25–34

Braekevelt CR, Thorlakson IJ (1993) Fine structure of the retinal pigment epithelium of the great horned owl (*Bubo virginianus*). Histol Histopathol 8(1):17–23

Braekevelt CR, Smith BJ, Smith SA (1996a) Fine structure of the retinal pigment epithelium of the barred owl (*Strix varia*). Histol Histopathol 11(1):71–77

Braekevelt CR, Smith SA, Smith BJ (1996b) Fine structure of the retinal photoreceptors of the barred owl (*Strix varia*). Histol Histopathol 11(1):79–88

Bravo H, Pettigrew JD (1981) The distribution of neurons projecting from the retina and visual cortex to the thalamus and *tectum opticum* of the barn owl, *Tyto alba*, and the burrowing owl, *Speotyto cunicularia*. J Comp Neurol 199(3):419–441

Budnik V, Mpodozis J, Varela FJ, Maturana HR (1984) Regional specialization of the quail retina: ganglion cell density and oil droplet distribution. Neurosci Lett 51(1):145–150

Campenhausen MV, Kirschfeld K (1998) Spectral sensitivity of the accessory optic system of the pigeon. J Comp Physiol A 183(1):1–6

Cowan WM, Powell TP (1963) Centrifugal fibres in the avian visual system. Proc R Soc Lond B Biol Sci 158:232–252

Cuthill IC, Partridge JC, Bennett ATD, Church SC, Hart NS, Hunt S (2000) Ultraviolet vision in birds. Adv Stud Behav 29:159–214

Dolan T, Fernández-Juricic E (2010) Retinal ganglion cell topography of five species of ground-foraging birds. Brain Behav Evol 75(2):111–121

Dontsov AE, Glickman RD, Ostrovsky MA (1999) Retinal pigment epithelium pigment granules stimulate the photo-oxidation of unsaturated fatty acids. Free Radic Biol Med 26(11–12):1436–1446

Edmonds DT (1996) A sensitive optically detected magnetic compass for animals. Proc Biol Sci 263(1368):295–298

Ehrlich D (1981) Regional specialization of the chick retina as revealed by the size and density of neurons in the ganglion cell layer. J Comp Neurol 195(4):643–657

El-Beltagy AEFB (2015) Light and electron microscopic studies on the pigmented epithelium and photoreceptors of the retina of common buzzard (*Buteo buteo*). Tissue Cell 47(1):78–85

Fischer AJ, Stell WK (1999) Nitric oxide synthase-containing cells in the retina, pigmented epithelium, choroid, and sclera of the chick eye. J Comp Neurol 405(1):1–14

Fritzsch B, Crapon de Caprona MD, Clarke PG (1990) Development of two morphological types of retinopetal fibers in chick embryos, as shown by the diffusion along axons of a carbocyanine dye in the fixed retina. J Comp Neurol 300(3):405–421

Gaffney MF, Hodos W (2003) The visual acuity and refractive state of the American kestrel (*Falco sparverius*). Vis Res 43(19):2053–2059

Gallego A, Baron M, Gayoso M (1975) Organization of the outer plexiform layer of the diurnal and nocturnal bird retinae. Vis Res 15:1027–1028

Goldsmith TH, Collins JS, Licht S (1984) The cone oil droplets of avian retinas. Vis Res 24(11):1661–1671

Hart NS (2001) The visual ecology of avian photoreceptors. Prog Retin Eye Res 20(5):675–703

Hart NS, Vorobyev M (2005) Modelling oil droplet absorption spectra and spectral sensitivities of bird cone photoreceptors. J Comp Physiol A Neuroethol Sens Neural Behav Physiol 191(4):381–392

Hart N, Partridge J, Cuthill II (1998) Visual pigments, oil droplets and cone photoreceptor distribution in the european starling (*Sturnus vulgaris*). J Exp Biol 201(Pt 9):1433–1446

Hart NS, Lisney TJ, Collin SP (2006) Cone photoreceptor oil droplet pigmentation is affected by ambient light intensity. J Exp Biol 209(Pt 23):4776–4787

Hayes BP, Holden AL (1983) The distribution of centrifugal terminals in the pigeon retina. Exp Brain Res 49(2):189–197

Hirsch J (1982) Falcon visual sensitivity to grating contrast. Nature 300:57–58

Ikushima M, Watanabe M, Ito H (1986) Distribution and morphology of retinal ganglion cells in the Japanese quail. Brain Res 376(2):320–334

Inzunza O, Bravo H, Smith RL, Angel M (1991) Topography and morphology of retinal ganglion cells in Falconiforms: a study on predatory and carrion-eating birds. Anat Rec 229(2):271–277

Jones MP, Pierce K Jr, Ward D (2007) Avian vision: a review of form and function with special consideration to birds of prey. J Exot Pet Med 16(2):69–87

Khattab F, Khattab FI, Fares N, Zaki A (2004) Retinal photoreceptor fine structure in some reptiles. EJHM 17:167–186

Kirschfeld K (1982) Carotenoid pigments: their possible role in protecting against photooxidation in eyes and photoreceptor cells. Proc R Soc Lond B Biol Sci 216(1202):71–85

Kolb H, Jones J (1982) Light and electron microscopy of the photoreceptors in the retina of the red-eared slider, *Pseudemys scripta elegans*. J Comp Neurol 209(4):331–338

Lamb TD (2009) Evolution of vertebrate retinal photoreception. Philos Trans R Soc Lond B Biol 364(1531):2911–2924

Lythgoe JN (1979) The ecology of vision. Clarendon Press, Oxford

Maier EJ, Bowmaker JK (1993) Colour vision in the passeriform bird, *Leiothrix lutea*: correlation of visual pigment absorbance and oil droplet transmission with spectral sensitivity. J Comp Physiol A 172:295–301

Martin GR (2012) Through birds' eyes: insights into avian sensory ecology. J Ornithol 153(1):23–48

Martin GR, Portugal SJ (2011) Differences in foraging ecology determine variation in visual fields in ibises and spoonbills (Threskiornithidae). IBIS 153(4):662–671

Meyer DB (1977) The avian eye and its adaptations. In: Crescitelli F (ed) Handbook of sensory physiology. Springer, Berlin, pp 549–612

Morgan IG, Miethke P, Li ZK (1994) Is nitric oxide a transmitter of the centrifugal projection to the avian retina? Neurosci Lett 168(1–2):5–7

Muntz WR (1972) Inert absorbing and reflecting pigments. In: Dartnall HJ (ed) Handbook of sensory physiology. Springer, Berlin, pp 529–595

Naito J, Chen Y (2004) Morphologic analysis and classification of ganglion cells of the chick retina by intracellular injection of lucifer yellow and retrograde labeling with Dil. J Comp Nuerol 469(3):360–376

Nalbach HO, Wolf-Oberhollenzer F, Remy M (1993) Exploring the image. In: Zeigler HP, Bischof HJ (eds) Vision, brain, and behavior in birds. MIT Press, Cambridge, pp 25–46

Pettigrew JE (1978) Comparison of the retinotopic organization of the visual wulst in nocturnal and diurnal raptors, with a note on the evolution of frontal vision. In: Cool SJ, Smith EL (eds) Frontiers in visual science, vol 8. Springer series in optical sciences. Springer, Berlin, pp 328–335

Rahman ML, Sugita S, Aoyama M, Sugita S (2006) Number, distribution and size of retinal ganglion cells in the jungle crow (*Corvus macrorhynchos*). Anat Sci Int 81(4):253–259

Rahman ML, Aoyama M, Sugita S (2007a) Regional specialization of the Tree Sparrow *Passer montanus* retina: ganglion cell density and oil droplet distribution. Ornithol Sci 6(2):95–105

Rahman ML, Aoyama M, Sugita S (2007b) Topography of retinal photoreceptor cells in the Jungle Crow (*Corvus macrorhynchos*)

with emphasis on the distribution of oil droplets. Ornithol Sci 6:29–38
Reymond L (1987) Spatial visual acuity of the falcon, *Falco berigora*: a behavioural, optical and anatomical investigation. Vision Res 27(10):1859–1874
Rodieck RW (1973) The vertebrate retina. W. H. Freeman and Company, San Francisco
Ruggeri M, Major JC, McKeown C, Knighton RW, Puliafito CA, Jiao S (2010) Retinal structure of birds of prey revealed by ultra-high resolution spectral-domain optical coherence tomography. Invest Ophtalmol Vis Sci 51(11):5789–5795
Schraermeyer U, Heimann K (1999) Current understanding on the role of retinal pigment epithelium and its pigmentation. Pigment Cell Res 12(4):219–236
Segovia Y, García M, Gómez-Torres MJ, Mengual R (2016) Ultrastructural study of retinal development in the turtle *Trachemys scripta elegans*. Zoomorphology 135:205–216
Seo JH, Haam YG, Park SW, Kim DW, Jeon GS, Lee C, Hwang CH, Kim YS, Cho SS (2001) Oligodendroglia in the avian retina: immunocytochemical demonstration in the adult bird. J Neurosci Res 65(2):173–183
Tancred E (1981) The distribution and sizes of ganglion cells in the retinas of five Australian marsupials. J Comp Neurol 196(4):585–603
Uchiyama H, Aoki K, Yonezawa S, Arimura F, Ohno H (2004) Retinal target cells of the centrifugal projection from the isthmo-optic nucleus. J Comp Neurol 476(2):146–153
Uga S, Smelser (1973) Comparative study of the fine structure of retinal Müller cells in various vertebrates. Invest Ophthalmol 12(6):434–448
Vorobyev M (2003) Coloured oil droplets enhance colour discrimination. Proc Biol Sci 270(1521):1255–1261
Vorobyev M, Osorio D (1998) Receptor noise as a determinant of colour thresholds. Proc Biol Sci 265(1394):351–358
Wagner HJ (1990) Retinal structure of fishes. In: Douglas RH, Djamgoz MB (eds) The visual system of fish. Springer Netherlands, London, pp 109–157
Walls GL (1942) The vertebrate eye and its adaptive radiation. Hafner Publising Company, New York
Walls GL, Judd HD (1933) The intra-ocular colour-filters of vertebrates. Br J Ophthalmol 17(11):641–675
Weller C, Lindstrom SH, De Grip WJ, Wilson M (2009) The area centralis in the chicken retina contains efferent target amacrine cells. Vis Neurosci 26(2):249–254
Wilby D, Toomey MB, Olsson P, Frederiksen R, Cornwall MC, Oulton R, Kelber A, Corbo JC, Roberts NW (2015) Optics of cone photoreceptors in the chicken (*Gallus gallus domesticus*). J R Soc Interface 12(111):20150591
Won MH, Kang TC, Cho SS (2000) Glial cells in the bird retina: immunochemical detection. Microsc Res Tech 50(2):151–160
Yau KW (1994) Phototransduction mechanism in retinal rods and cones. The Friedenwald Lecture. Invest Ophthalmol Vis Sci 35(1):9–32
Young RW, Bok D (1979) Metabolism of the pigment epithelium. In: Zinn KM, Marmot MF (eds) The retinal pigment epithelium. Harvard University Press, Cambridge, pp 103–123
Young SR, Martin GR (1984) Optics of retinal oil droplets: a model of light collection and polarization detection in the avian retina. Vis Res 24(2):129–137